HAL
open science

Synthesis and evaluation of zirconium-89 labelled and long-lived GLP-1 receptor agonists for PET imaging

Christian Borch Jacobsen, René Raavé, Marie Østergaard Pedersen, Pierre Adumeau, Mathieu Moreau, Ibai E. Valverde, Inga Bjørnsdottir, Jesper Bøggild Kristensen, Mette Finderup Grove, Kirsten Raun, et al.

To cite this version:

Christian Borch Jacobsen, René Raavé, Marie Østergaard Pedersen, Pierre Adumeau, Mathieu Moreau, et al.. Synthesis and evaluation of zirconium-89 labelled and long-lived GLP-1 receptor agonists for PET imaging. Nuclear Medicine and Biology, 2020, 82-83, pp.49-56. 10.1016/j.nucmedbio.2019.11.006 . hal-03004102

HAL Id: hal-03004102

https://hal.science/hal-03004102v1

Submitted on 17 Nov 2020

HAL is a multi-disciplinary open access archive for the deposit and dissemination of scientific research documents, whether they are published or not. The documents may come from teaching and research institutions in France or abroad, or from public or private research centers.

L'archive ouverte pluridisciplinaire **HAL**, est destinée au dépôt et à la diffusion de documents scientifiques de niveau recherche, publiés ou non, émanant des établissements d'enseignement et de recherche français ou étrangers, des laboratoires publics ou privés.

Nuclear Medicine and Biology 82–83 (2020) 49–56

Contents lists available at ScienceDirect

Nuclear Medicine and Biology

journal homepage: www.elsevier.com/locate/nucmedbio

Synthesis and evaluation of zirconium-89 labelled and long-lived GLP-1 receptor agonists for PET imaging

Christian Borch Jacobsen [a,c,*], René Raavé [d], Marie Østergaard Pedersen [a], Pierre Adumeau [e], Mathieu Moreau [e], Ibai E. Valverde [e], Inga Bjørnsdottir [b], Jesper Bøggild Kristensen [c], Mette Finderup Grove [b], Kirsten Raun [b], James McGuire [b], Victor Goncalves [e], Sandra Heskamp [d], Franck Denat [e], Magnus Gustafsson [a,**]

[a] Global Research Technologies, Novo Nordisk A/S, Denmark
[b] Global Drug Discovery, Novo Nordisk A/S, Denmark
[c] Isotope Chemistry, CMC Development, Novo Nordisk A/S, Denmark
[d] Department of Radiology and Nuclear Medicine, Radboudumc, Radboud Institute for Molecular Life Sciences, Nijmegen, the Netherlands
[e] Institut de Chimie Moléculaire de l'Université de Bourgogne, UMR CNRS 6302, Université Bourgogne Franche-Comté, France

ARTICLE INFO

Article history:
Received 17 October 2019
Received in revised form 25 November 2019
Accepted 28 November 2019

Keywords:
GLP-1
Zirconium-89
Molecular imaging
PET
Bioconjugation
Radiolabelling

ABSTRACT

Introduction: Lately, zirconium-89 has shown great promise as a radionuclide for PET applications of long circulating biomolecules. Here, the design and synthesis of protracted and long-lived GLP-1 receptor agonists conjugated to desferrioxamine and labelled with zirconium-89 is presented with the purpose of studying their *in vivo* distribution by PET imaging. The labelled conjugates were evaluated and compared to a non-labelled GLP-1 receptor agonist in both *in vitro* and *in vivo* assays to certify that the modification did not significantly alter the peptides' structure or function. Finally, the zirconium-89 labelled peptides were employed in PET imaging, providing visual verification of their *in vivo* biodistribution.
Methods: The evaluation of the radiolabelled peptides and comparison to their non-labelled parent peptide was performed by *in vitro* assays measuring binding and agonistic potency to the GLP-1 receptor, physicochemical studies aiming at elucidating change in peptide structure upon bioconjugation and labelling as well as an *in vivo* food in-take study illustrating the compounds' pharmacodynamic properties. The biodistribution of the labelled GLP-1 analogues was determined by *ex vivo* biodistribution and *in vivo* PET imaging.
Results: The results indicate that it is surprisingly feasible to design and synthesize a protracted, zirconium-89 labelled GLP-1 receptor agonist without losing *in vitro* potency or affinity as compared to a non-labelled parent peptide. Physicochemical properties as well as pharmacodynamic properties are also maintained. The biodistribution in rats shows high accumulation of radiolabelled peptide in well-perfused organs such as the liver, kidney, heart and lungs. The PET imaging study confirmed the findings from the biodistribution study with a significant high uptake in kidneys and presence of activity in liver, heart and larger blood vessels.
Conclusions and advances in knowledge: This initial study indicates the potential to monitor the *in vivo* distribution of long-circulating incretin hormones using zirconium-89 based PET.
© 2019 The Authors. Published by Elsevier Inc. This is an open access article under the CC BY-NC-ND license (http://creativecommons.org/licenses/by-nc-nd/4.0/).

1. Introduction

Treatment with short- and long-acting glucagon-like peptide 1 receptor (GLP-1R) agonists has become a successful therapy for type 2 diabetes providing effective glycemic control, improved beta-cell function, body weight loss, and lowering of systolic blood pressure [1]. Exenatide, with a subcutaneous half-life of 2.4 h in humans for twice daily administration, was the first approved compound in 2005 [2], followed by once-daily liraglutide in 2009 with a subcutaneous half-life of 13–15 h [3]. The next generation of GLP-1R agonists as exemplified by albiglutide, dulaglutide, and semaglutide, were developed to support once-weekly dosing [4–6]. Albiglutide consists of two GLP-1 molecules fused to human serum albumin and displays a half-life of around 6–8 days [4], while dulaglutide is a GLP-1 analogue fused to a Fc-fragment with a half-life of 90 h [5]. In 2015, Lau *et al.* reported a series of acylated GLP-1 peptides where increased albumin affinity relative to liraglutide also led to a once-weekly profile with a biological half-life in humans of 165 h [6]. The long half-life could be reached

* Correspondence to: Christian Borch Jacobsen, Isotope Chemistry, CMC Development, Novo Nordisk A/S, Novo Allé, DK-2880 Bagsværd, Denmark.
** Correspondence to: Magnus Gustafsson, Global Research Technologies, Novo Nordisk A/S, Novo Nordisk Park, DK-2760 Måløv, Denmark.
E-mail addresses: cbjc@novonordisk.com (C.B. Jacobsen), mbfg@novonordisk.com (M. Gustafsson).

https://doi.org/10.1016/j.nucmedbio.2019.11.006
0969-8051/© 2019 The Authors. Published by Elsevier Inc. This is an open access article under the CC BY-NC-ND license (http://creativecommons.org/licenses/by-nc-nd/4.0/).

through a reversible binding to albumin through a fatty acid moiety attached to a lysine residue in position 26.

For the direct imaging of the *in vivo* distribution and accumulation of selective receptor-targeting peptide-based agents, non-invasive molecular imaging techniques such as positron emission tomography (PET), single photon emission computed tomography (SPECT), magnetic resonance imaging (MRI), or fluorescence imaging, have attracted considerable attention, particularly for cancer detection [7]. Lately, zirconium-89 has shown great promise as a radionuclide for PET applications of long circulating biomolecules due to its long physical half-life of 78.4 h. Furthermore, the low energy of the emitted positrons can provide high resolution images [8–11].

The use of radiolabelled GLP-1R agonists did indeed start over a decade ago in the field of nuclear oncology [12]. GLP-1R agonists, such as exendin 3 and 4, have attracted attention in the medical field for the detection of malign insulinomas that overexpress the GLP-1R and the localization and quantification of subcutaneously implanted beta cells masses [13]. GLP-1 radiolabelling using iodine-123 for imaging has been reported, but the short half-life of the isotope, as compared to the biological half-life of modern GLP-1 receptor agonists, and the report of instability of the radiotracer *in vivo*, makes this technique less attractive for determining the fate of long circulating incretin hormone analogues [14]. Azad *et al.* and Brom *et al.* successfully used SPECT for pancreatic beta cell imaging in connection with functionalized GLP-1 analogues bearing an indium-111 chelate [15,16], but the low spatial resolution of this technique is a possible concern. In order to benefit from both the superior spatial resolution of PET imaging, and the long half-life of zirconium-89 that allows late time-point imaging acquisitions, another option for studying circulating incretin analogues could be to use zirconium-89 based PET imaging as positively reported by Bauman *et al.* in imaging of small-sized insulinomas with radiolabelled exendin-4 analogues [8].

Here, we report the first synthesis and characterization of a fatty acid substituted GLP-1 analogue functionalized with the siderophore desferrioxamine (DFO), a chelator enabling radiolabelling with zirconium-89, for studies of its *in vivo* distribution by PET imaging. To investigate whether the modification influences the peptide's overall structure and function, the radiotracer was synthesized, characterized and compared with a non-labelled parent GLP-1 analogue in various physicochemical, *in vitro* and *in vivo* assays. Through these experiments we aimed at determining if the radiotracer is a viable candidate for the indirect verification of the *in vivo* distribution of its non-labelled parent peptide. Finally, the distribution of the radiotracer was evaluated by *ex vivo* biodistribution and *in vivo* PET imaging studies.

2. Results and discussion

2.1. Design and synthesis of functionalized GLP-1 analogues

As the radiotracer must be modified with both a fatty acid side-chain and a DFO-based chelator, one of the important design criteria in our study was to identify a disubstituted GLP-1 analogue with sustained structural stability and strong GLP-1R binding. Furthermore, the analogue should have strong albumin binding properties to increase biological half-life and be functionally active at the GLP-1R to a similar extent as the unlabelled parent GLP-1R agonist.

Structure-activity information of fatty acid substituted analogues has been disclosed in earlier studies [17–19], and one of the conclusions from these reports were that GLP-1R agonists tolerate a fatty acid protractor in positions 16, 22, 26, 37 or in an extended C-terminal position without compromising receptor binding or activation. Similar conclusions were drawn by another group on designed mono-functionalized GLP-1 7-36/37 with a [^{111}In]In-DOTA complex, with a preferred modification position on K^{37} [15].

Double substituted analogues on the other hand were found to be substantially less potent [18]. As such, one of the initial main challenges to overcome, was to design an analogue with minimal interference between the two attached groups (side-chain and chelate) and, at the same time, avoid disturbance of critical amino acid residues involved in receptor interaction.

The starting point was peptide **1** (Fig. 1), with a binding affinity (IC_{50}) of 0.28 nM and an agonistic potency (EC_{50}) of 89.8 pM. As comparison, native GLP-1 has an EC_{50} of 5.0 pM in the same assay. The N-terminus was stabilized against enzymatic degradation by substituting the histidine for desamino-histidine. Based on the available information (see Fig. 1), we envisioned position 26 and the C-terminal region to be suitable positions for the second attachment (*i.e.* of the metal chelator DFO). To avoid large interference with the side-chain, with concomitant reduced affinity to albumin, two analogues that contained a C-terminal GGSK extension (GLP-1 7-41 analogues), with the metal chelate positioned in K^{41}, were synthesized (see Fig. 2 and Supplementary information page S6 for structures).

The GLP-1 analogues were synthesized by solid-phase peptide synthesis (SPPS) using a standard Fmoc protection strategy as exemplified by peptide **4** (Fig. 2). The use of Fmoc-Lys(Mtt)-OH and Fmoc-Lys(Boc)-OH ensured the site-specific incorporation of the albumin binding motif and the metal chelator. The Mtt protection group was selectively cleaved using 1,1,1,3,3,3-hexafluoroisopropanol (HFIP) and the fatty acid side-chain was sequentially built up using SPPS (Fig. 2, Step 1). TFA-induced cleavage of the peptide from the resin with subsequent global deprotection ensured the liberation of the free amine handle on the lysine residue (Fig. 2, Step 2). After purification, the conjugation between the peptide and the chelator was carried out in a carbonate buffered solution (Fig. 2, Step 3). At slightly elevated temperatures (50 °C) and alkaline pH, the coupling was complete within 3 h by adding three equivalents of chelator to the stirred peptide solution. The desired conjugate was then easily purified by preparative HPLC on a C18 column and subsequently labelled with Zr^{4+} to generate **Zr-DFO-4** or [^{89}Zr]Zr^{4+} to give **[^{89}Zr]Zr-DFO-4**.

For this study, we chose to employ the recently reported squaramide-based linker [20] over the more conventional hydrophobic thiourea-based linker formed from 1,4-phenylene diisothiocyante [11,21]. As previously described in the literature [20], we also observed a small increase in stability using the squaramide linker compared to the 1,4-phenylene diisothiocyanate-based conjugate (See Supplementary information page S11). Yet more importantly, we observed that the solubility of the conjugated peptides at physiological pH is enhanced to an extent that greatly decreases the cumbersomeness often reported to be an issue when conjugating DFO-based moieties to peptides with 1,4-phenylene diisothiocyanate [9,20].

For our initial *in vitro*, physicochemical, and *in vivo* studies (*vide infra*), we inserted non-radioactive zirconium into the conjugates simply by adding a solution of $ZrCl_4$ directly to the HPLC fractions to provide the conjugated peptides **Zr-DFO-2**, **Zr-DFO-3**, **Zr-DFO-4** and **Zr-DFO*-5** in good purity after purification.

2.2. In vitro and physicochemical characterization

Our initial studies aimed at identifying a conjugation position within peptide **1** where the addition of DFO did not significantly alter the peptides structure or function *in vitro*. As mentioned, previous studies with other GLP-1 analogues have shown that the addition of a fatty acid-based albumin-binding protractor to a lysine in position 37, does not significantly interfere with the receptor affinity [6], as exemplified in Table 1 with peptide **1**. The affinity of compound **1** for the human GLP-1 receptor in the absence of albumin was determined by a competition assay measuring the inhibition of iodine-125 labelled native GLP-1 (7-37) binding, and provided an IC_{50} value of 0.33 nM. A functional luciferase assay was used to estimate the potency of the same compound on the human GLP-1 receptor in presence of albumin resulting of an EC_{50} value of 89.8 pM (see Supplementary information page S7).

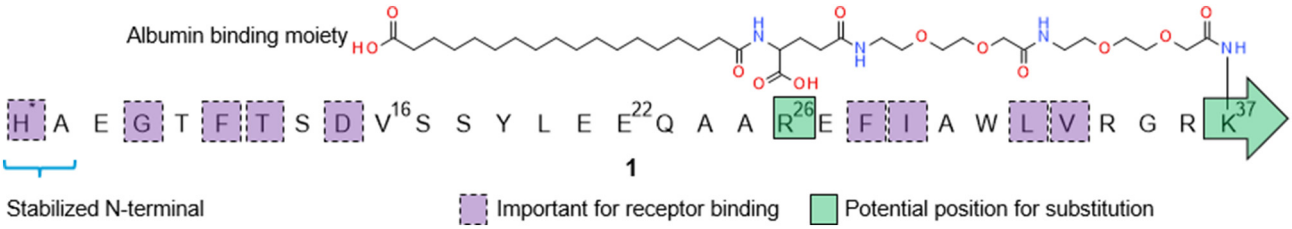

Fig. 1. The structure of GLP-1 receptor agonist **1** with indications of amino acids being viable positions for modification. H* indicates desamino-histidine.

Conjugating the DFO moiety to an internal residue resulted in a significant loss of both affinity and potency, as illustrated with compound **Zr-DFO-2** having IC_{50} and EC_{50} values of 4.20 nM and >1928 pM, respectively. As illustrated by **Zr-DFO-3**, switching the position of the two groups had no advantageous effect with an IC_{50} of 9.50 nM and an EC_{50} of 1144 pM. The poor binding efficiency for GLP-1R for **Zr-DFO-2** and **Zr-DFO-3** were particularly pronounced in the presence of HSA. Placing both the side-chain and chelator at the C-terminal gave a more satisfactory results as indicated with analogue **Zr-DFO-4**. This compound has the same 30 amino acids as **1** in the N-terminus but possesses a C-terminal GGSK-extension to which the DFO chelator is attached by the C-terminal lysine residue in position 41 through the squaramide linker. **Zr-DFO-4** maintained the excellent affinity and potency of its non-conjugated parent **1** as its IC_{50} and EC_{50} in the same assays were

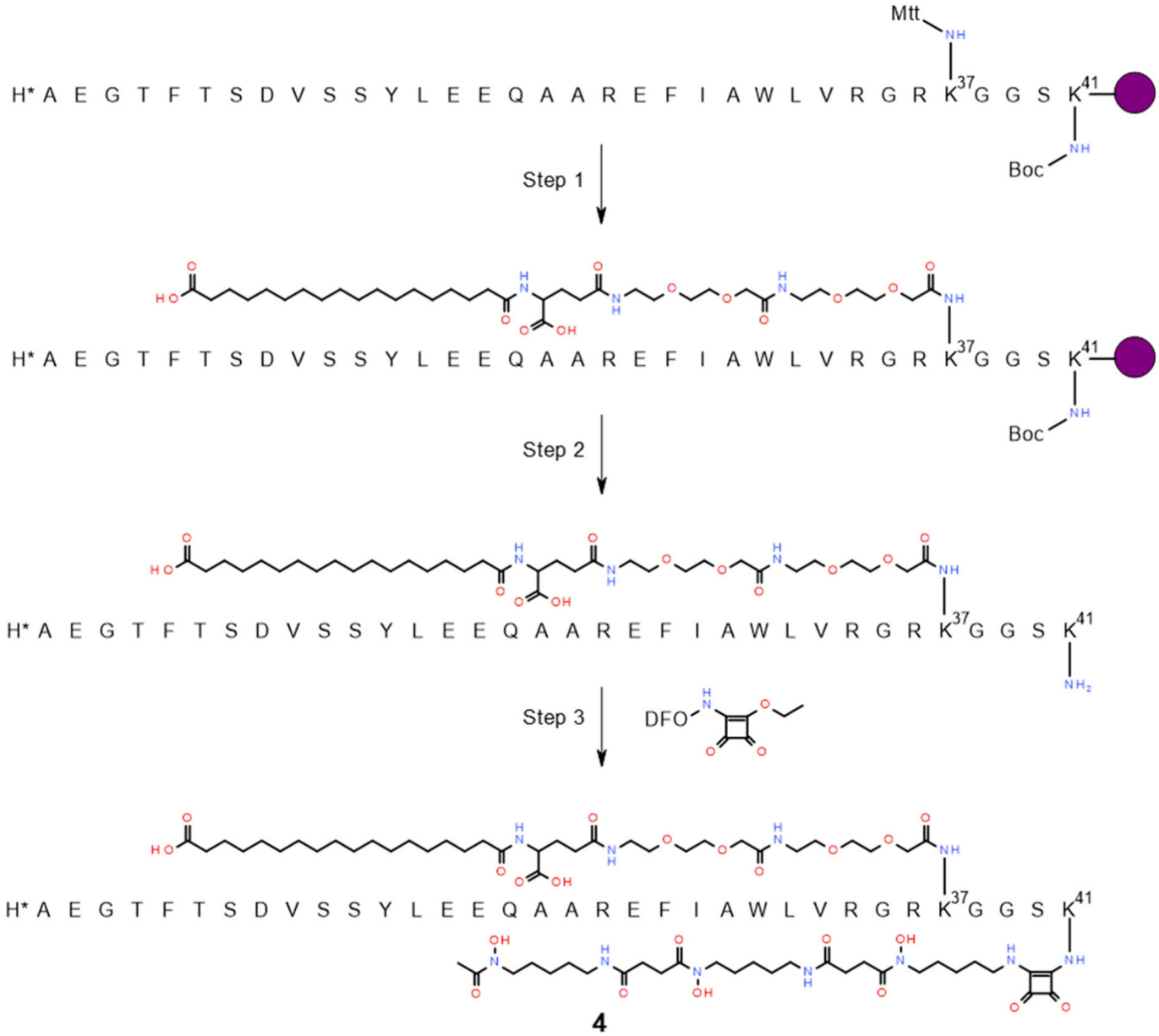

Fig. 2. Synthesis of the GLP-1 analogues by SPPS using Fmoc strategy with **4** shown as an example. Step 1: *N*-Mtt deprotection and sequential assembly of albumin binding moiety. Step 2: Cleavage and global deprotection with TFA. Step 3: Solution phase coupling of DFO-squaric acid reagent. Mtt = 4-methyltrityl.

Table 1
In vitro affinity and potency for the human GLP-1 receptor for substituted (GLP-1)7-37 and (GLP-1)7-41 analogues (**1**, **Zr-DFO-2**, **Zr-DFO-3**, **Zr-DFO-4**, and **Zr-DFO*-5**).

Analogue	C-terminal extension	Chelate position	Side-chain position	GLP-1R binding (IC_{50}, nM)		Ratio 2%/0% HSA	GLP-1R potency (EC_{50}, pM) 1% HSA
				0% HSA	2% HSA		
1	n.a.	n.a.	37	(C)0.33 ± 0.08	(C)69.8 ± 16.7	212 ± 72.0	(B)89.8 ± 12.2
Zr-DFO-2	n.a.	(D)26	37	(B)4.20 ± 0.40	(B)>1000	>238	(A)1928
Zr-DFO-3	n.a.	(D)37	26	(B)9.50 ± 1.50	(B)>1000	>105	(A)1144
Zr-DFO-4	GGSK	(D)41	37	(C)0.61 ± 0.14	(C)112 ± 33.3	183 ± 69.0	(B)124 ± 56.9
Zr-DFO*-5	GGSK	(E)41	37	(B)0.83 ± 0.28	(B)159 ± 52.3	192 ± 90.3	(A)379

GLP-1 receptor binding in the presence of 0% or 2% albumin (HSA) using plasma membranes from BHK cells expressing the human GLP-1R and *in vitro* potency measured in BHK cells that express both the human GLP-1R and a luciferase reporter system. Numbers are mean ± standard deviation. (A) $n = 1$, (B) $n = 2$, (C) $n = 4$. Chelator is (D) = DFO or (E) = DFO*.

measured to be 0.61 nM and 124 pM, respectively. Similar positive data were achieved with analogue **Zr-DFO*-5**, where DFO was exchanged for DFO*, a recently reported promising metal chelator suitable for zirconium-89 complexation [22]. These results underline the importance of separating the chelator from the binding sequence of the peptide, particularly in the case of large-sized chelators such as DFO and analogues hereof.

An indirect method for estimating the albumin binding was used to investigate the affinity of the peptide for albumin, a prerequisite for prolonged plasma circulation [6]. The IC_{50} of analogues **Zr-DFO-2**, **Zr-DFO-3**, **Zr-DFO-4**, and **Zr-DFO*-5** were measured in the presence of high (2%) or low (0%) concentration of HSA and compared with **1**. Similar ratios between the analogues and **1** were observed, particularly for **Zr-DFO-4** and **Zr-DFO*-5**, indicating that these analogues bind reasonably to albumin and to a similar extent as parent GLP-1 analogue **1**.

To further evaluate whether the addition of the Zr-DFO-chelate caused significant alterations of the structural integrity of the GLP-1R agonists, **1**, **Zr-DFO-2**, and **Zr-DFO-4** were compared using a combination of circular dichroism (CD) spectroscopy to evaluate differences in secondary structure, and dynamic light-scattering (DLS) to determine if self-association of the peptides was altered (Table 2).

Native GLP-1 has been reported to form a helical structure in solution as seen by NMR [23] with the degree of helicity being dependent on the solution conditions [24], and several publications have shown that the α-helix is retained within the receptor-binding pocket [25,26] illustrating the importance of maintaining a high helicity after conjugation to DFO.

CD spectra (Fig. 3) showed that all three peptides adopt an α-helical structure, as seen by the two negative peaks at 208 nm and 222 nm in combination with the large positive peak around 190 nm [27]. The GLP-1R agonist without DFO (**1**) was calculated to have 36% of its backbone in an alpha helix conformation and the same was seen for analogue **Zr-DFO-2** with the DFO-chelate placed in position 26. The extended analogue **Zr-DFO-4** seems to have a slightly higher degree of helicity (46%) under the same conditions.

From DLS we observed that **1** and **Zr-DFO-2** form similarly sized oligomers of 1.94 ± 0.06 nm and 1.98 ± 0.06 nm, respectively, whereas **Zr-DFO-4** forms slightly larger oligomers of 2.30 ± 0.01 nm. The slightly larger size and increased helicity correspond well with the greater size of the peptide, due to the C-terminal extension, and illustrates that the modification with the DFO chelate does not alter the structure nor self-association of the lipidated GLP-1 analogues.

The conclusion we draw from these initial results is that conjugation of the DFO chelator to a lysine residue in the C-terminal extension of **Zr-DFO-4** is the most viable way of modifying the peptide **1** for labelling with zirconium-89 without significantly altering the peptides structure or function. We thus next endeavored to find out whether this modification could also be performed without influencing the pharmacodynamic (PD) properties of the GLP-1 analogue *in vivo*.

Table 2
In vitro affinity for the GLP-1 receptor and physicochemical properties for each of the compounds **1**, **Zr-DFO-2**, and **Zr-DFO-4**.

Analogue	α-Helical content (%)	Hydrodynamic radius (nm)	GLP-1R binding (IC_{50}, nM, 2% HSA)
1	36	1.94 ± 0.06	69.8 ± 16.7
Zr-DFO-2	36	1.98 ± 0.06	>1000
Zr-DFO-4	46	2.30 ± 0.01	112 ± 33.3

GLP-1 receptor binding at 2% albumin (HSA) using plasma membranes from BHK cells expressing the human GLP-1R. Numbers are mean ± standard deviation.

2.3. In vivo pharmacodynamics

In addition to their incretin effect, GLP-1 analogues are well-recognized as potent agents for reducing appetite and inducing weight loss [28]. In order to determine the pharmacodynamic potency of **1** *in vivo* and to test whether this potency is maintained after the conjugation to DFO as in **Zr-DFO-4**, we subjected both compounds to a food-intake study.

A total of 32 Sprague Dawley rats on a reversed day-night cycle were randomized and divided into groups receiving either only vehicle (control group) or vehicle with two different concentrations of peptide (**1** or **Zr-DFO-4** in either 10 or 100 nmol/kg) by subcutaneous injection (see Supplementary Information page S9). Fig. 4 illustrates the accumulated mean food-intake in each of the 5 groups from 24 h prior to 48 h after administration.

Mean food-intake was similar in all 5 groups until the administration of the peptides or vehicle at time 0. After administration, the control group receiving only vehicle maintains a food-intake averaging at just over 20 g per day per rat. The remaining groups receiving **1** or **Zr-DFO-4** in the vehicle show a rapid reduction in food-intake with no significant difference between **1** and **Zr-DFO-4** in either dose after 24 h. Later timepoints indicate that the effect of **Zr-DFO-4** wears off faster than for **1**, presumably due to a slight difference in pharmacokinetic properties.

Overall, however, the pharmacodynamic profile of both compounds is comparable. Combined with the *in vitro* and physical chemical data (*vide supra*) this demonstrates that the GLP-1 analogue **1** can be modified, with a DFO-type chelator through a squaramide-based linker to form **Zr-DFO-4**, maintaining the overall structure and function of the peptide both *in vitro* and *in vivo*. As such, this modified peptide is

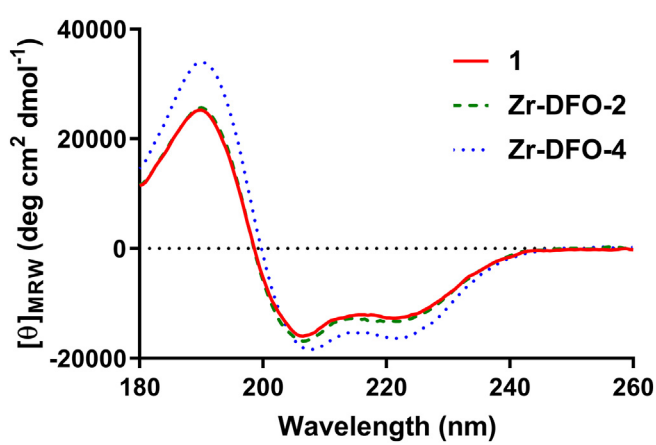

Fig. 3. Far UV CD spectra at 25 °C of 20 μM **1**, **Zr-DFO-2**, and **Zr-DFO-4** in 10 mM phosphate buffer, pH 7.4.

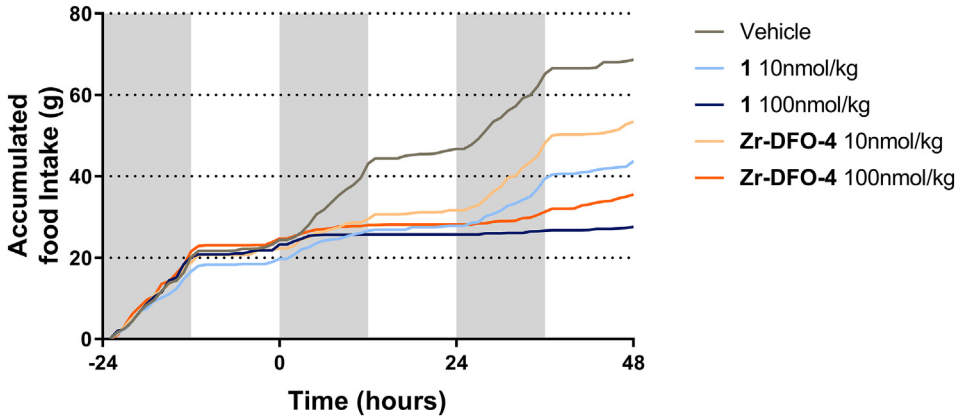

Fig. 4. Accumulated food-intake in average g/rat for rats dosed subcutaneous with either vehicle or **1** or **Zr-DFO-4** in vehicle in doses of either 10 or 100 nmol/kg rat. The graphs are shown without statistical error for simplicity but can be found with standard deviations in the Supplementary information page S10.

seemingly a viable candidate for the indirect verification of the *in vivo* distribution of **1**. We next aimed to investigate this through zirconium-89 labelling and subsequent biodistribution and PET imaging studies.

2.4. Radiolabelling, pharmacokinetics and biodistribution of radiolabelled **[^{89}Zr]Zr-DFO-4** *and* **[^{89}Zr]Zr-DFO*-5**

In order to assess the biodistribution and blood kinetics of radiolabelled peptides, we performed the radiolabelling by adding a solution of [^{89}Zr]Zr(oxalate)$_2$ to a buffered solution containing the conjugated peptide. After having determined the radiolabelling efficiency (>98,5%, 5 MBq/nmol), the stability of the conjugates was tested. We decided to include the peptide **[^{89}Zr]Zr-DFO*-5** with a DFO*-chelator in position 41. The DFO*-chelator was previously demonstrated to form a more stable chelate with zirconium-89 compared to DFO, resulting in less accumulation of the free radionuclide in bone [29,30,31]. As indicated in Fig. 5, EDTA challenge showed increased stability for DFO*, as expected based on literature.

The integrity of **[^{89}Zr]Zr-DFO-4** decreased to 70%, while **[^{89}Zr]Zr-DFO*-5** remained >95% intact after seven days. Also, the stability in human plasma of the two complexes was investigated, and in this assay both **[^{89}Zr]Zr-DFO-4** and **[^{89}Zr]Zr-DFO*-5** remained stable over seven days.

Slight differences in blood kinetics and biodistribution between **[^{89}Zr]Zr-DFO-4** and **[^{89}Zr]Zr-DFO*-5** were also observed (Fig. 6). The blood concentration is lower for **[^{89}Zr]Zr-DFO*-5** at the first measurement (15 min), suggesting a more rapid clearance from the circulation directly after injection of radioconjugate **[^{89}Zr]Zr-DFO*-5** compared to **[^{89}Zr]Zr-DFO-4**. However, from this point and onwards, **[^{89}Zr]Zr-DFO-4** clears with a similar kinetics as **[^{89}Zr]Zr-DFO*-5**. As seen from Fig. 6, the concentration trends towards the expected exponential dependence on time with 5–10% ID/g still present in the blood after 4 h.

As expected from an albumin-binding peptide, the biodistributions of the two compounds mainly show accumulation in well-perfused blood-filled organs as the liver, kidneys, heart and lungs at 4 h after injection (Fig. 7a). The high uptake in the kidney could result from the fact that these contain inherent expression of GLP-1 receptors in rat [16] and are a main pathway of excretion once the GLP-1 analogue is released from albumin. However, the level of radioactivity in the kidney in this study is lower than expected based on earlier reports [8]. One plausible explanation could be that albumin partly rescues the radiolabelled peptides from the megalin receptor-mediated uptake during proximal tubular reabsorption previously reported [32,33], and restore the GLP-1R agonists into systemic circulation.

As a consequence of the lower blood values of **[^{89}Zr]Zr-DFO*-5**, uptake in all well-perfused organs is lower for this compound (Fig. 7a). However, when looking at the organ-to-blood ratios (Fig. 7b), these differences are less apparent, indicating that the differences observed for the activity concentrations in well-perfused organs are indeed caused by the differences in blood concentration. The lung, duodenum, colon, liver and kidney showed a statistically significant higher organ-to-blood ratio for **[^{89}Zr]Zr-DFO*-5** compared to **[^{89}Zr]Zr-DFO-4**, of which the latter two may partly explain lower blood values compared to the DFO analogue by higher liver metabolism and excretion through the

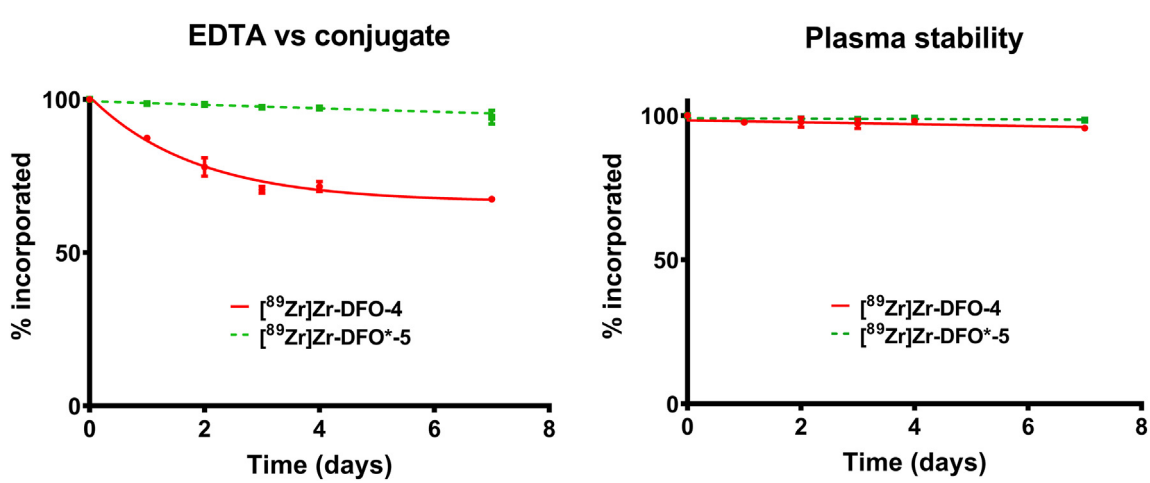

Fig. 5. Stability of **[^{89}Zr]Zr-DFO-4** (DFO chelate) and **[^{89}Zr]Zr-DFO*-5** (DFO* chelate) in the presence of 1000 equivalents of EDTA in PBS buffer at 37 °C or in human plasma. Error bars represent standard deviations ($n = 3$).

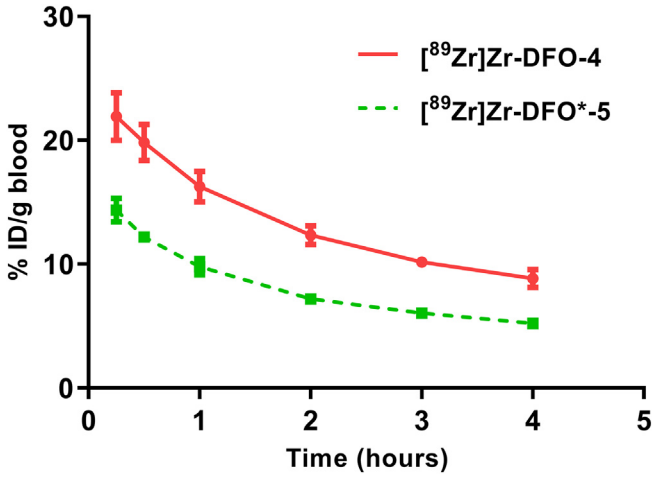

Fig. 6. Blood kinetics of the ^{89}Zr-labelled peptides conjugated to DFO (**[^{89}Zr]Zr-DFO-4**) or DFO* (**[^{89}Zr]Zr-DFO*-5**). Each rat received 1 nmol of conjugate (5 MBq of ^{89}Zr). Error bars represent standard deviations ($n = 5$).

kidney. Other factors that could contribute to the difference in early PK could be difference in solubility and binding kinetics to rat serum albumin between **[^{89}Zr]Zr-DFO-4** and **[^{89}Zr]Zr-DFO*-5**.

Bone uptake was lower for the DFO-analogue than often seen with this type of chelator, most likely because the *in vivo* release of zirconium-89 from DFO and subsequent accumulation in mineral bone is usually observed >72 h post injection [29]. When looking at organ-to-blood ratios, the overall picture is similar for the two radioconjugates.

PET imaging confirmed the findings of the *ex vivo* biodistribution study; high kidney uptake, with presence of the zirconium-89 labelled compounds in the liver and in circulation as observed by activity in the heart and large vessels (Fig. 8). An interesting observation is the uptake in a specific area in the upper abdominal area (marked with an asterisk in Fig. 8), most likely this is a specific part of the duodenum or small intestine, which was not identified by the *ex vivo* biodistribution study. A substantial accumulation of radioactivity in the renal cortex was also observed in the sagittal section through the organ (Fig. 8, sagittal view). A more detailed overview of the PET results can be found in Videos 1 and 2.

Overall, the PET imaging study, confirmed the findings from the *ex vivo* biodistribution study, thus providing a method for visual verification of the distribution of a GLP-1 analogue.

3. Conclusions

Long-circulating GLP-1R peptide agonists with a DFO-type chelate were synthesized and labelled with Zr^{4+} (**Zr-DFO-4** and **Zr-DFO*-5**) and [^{89}Zr]Zr^{4+} (**[^{89}Zr]Zr-DFO-4** and **[^{89}Zr]Zr-DFO*-5**). The *in vitro* and physicochemical characteristics of the DFO-bearing compounds were similar to the parent peptide without DFO chelate and it induced a similar reduction in food-intake in a rat pharmacodynamic model. The biodistribution of **[^{89}Zr]Zr-DFO-4** and **[^{89}Zr]Zr-DFO*-5** in rats show high accumulation of radiolabelled peptide in well-perfused organs such as the liver, kidney, heart and lungs. The PET imaging study confirmed

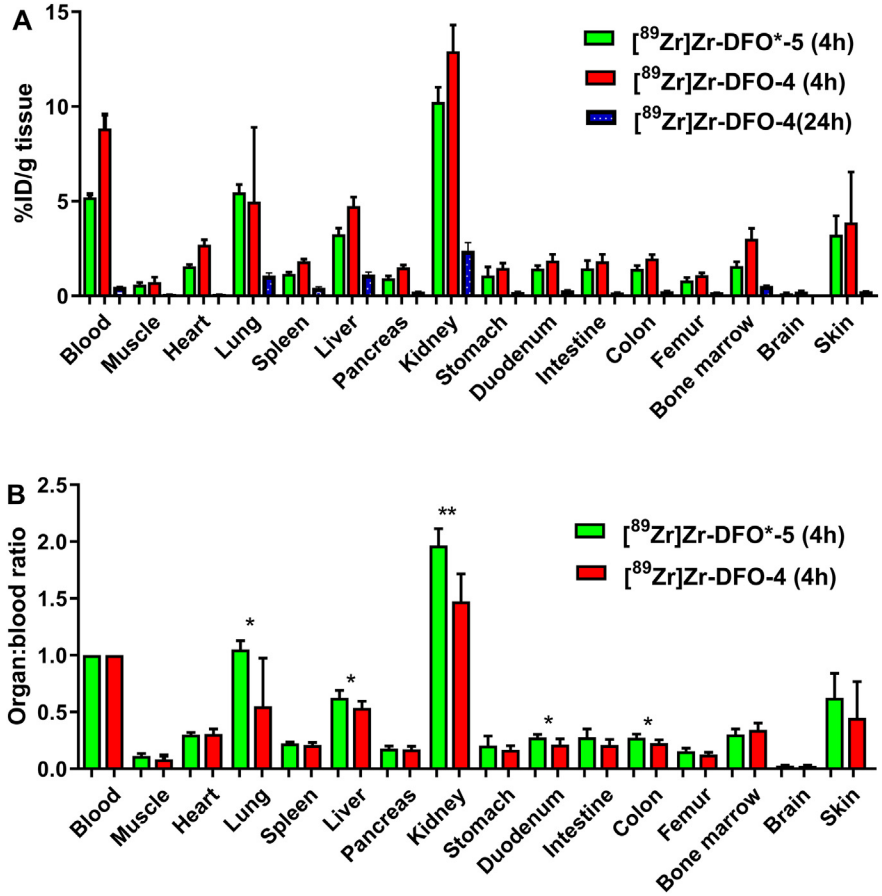

Fig. 7. A: *Ex vivo* biodistribution depicted as % injected dose/gram tissue (%ID/g) of the labelled peptides conjugated to DFO (**[^{89}Zr]Zr-DFO-4**) or DFO* (**[^{89}Zr]Zr-DFO*-5**), 4 or 24 h after administration in healthy rats. B: Organ to blood ratio of the biodistribution at 4 h after injection. Bars represent mean with standard deviation (For 4 h, $n = 5$; for 24 h, $n = 3$). $^{*}p < 0.05$; $^{**}p < 0.01$.

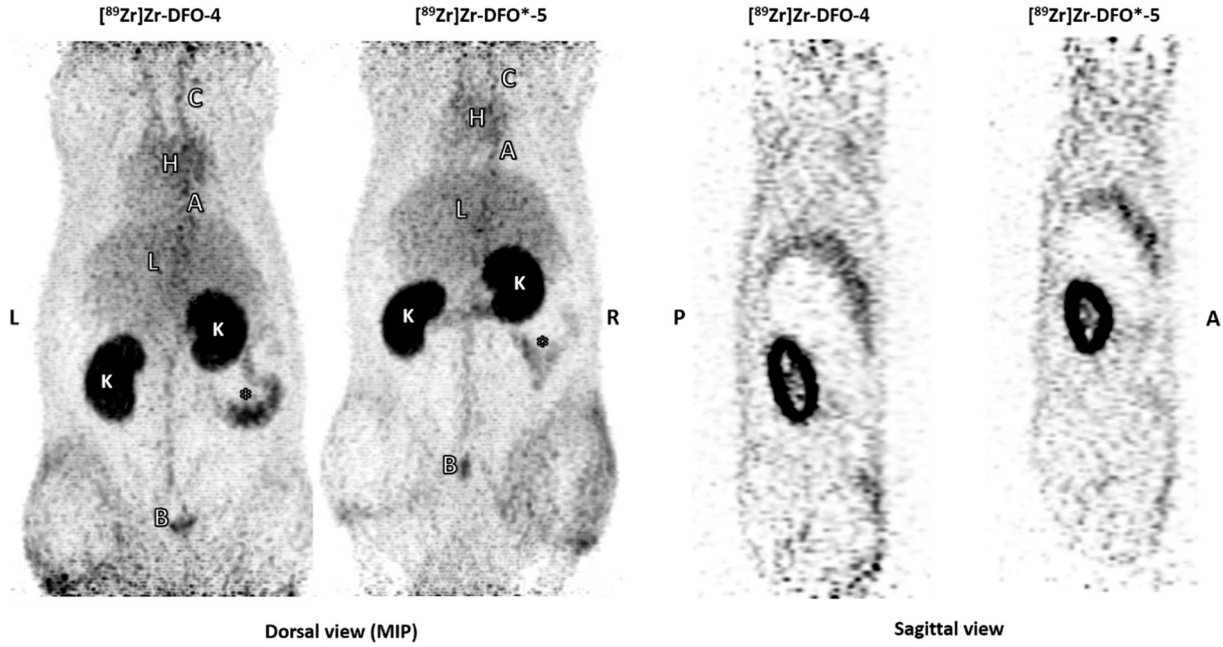

Fig. 8. Dorsal maximum intensity projection (MIP) and sagittal view PET images of rats injected with 5 MBq (1 nmol) ^{89}Zr-labelled peptides conjugated to DFO or DFO* 4 h after administration. A = aorta, B = bladder, C = carotic artery, H = heart, K = kidney, L = liver, and * = duodenum or small intestine. L = left, R = right. P = posterior, A = Anterior.

the findings from the biodistribution study with a significant high uptake in kidneys and presence of activity in liver, heart and larger blood vessels. This promising initial study indicates the potential to monitor the *in vivo* distribution of long-circulating incretin hormones using zirconium-89 based PET. As the expected biological half-life of fatty acid-substituted GLP-1 analogues such as **1** and **[^{89}Zr]Zr-DFO-4** are much longer in humans than in rats [34], the long physical half-life of zirconium-89 (78.4 h) enables future human studies with these molecules.

4. Materials and methods

4.1. Peptide synthesis

All non-modified peptides were synthesized using standard solid-phase Fmoc procedures on SymphonyX (Gyros Protein Technologies Inc.). Wang resins preloaded with the C-terminal amino acid were employed. The lysine to be modified with the fatty acid-based sidechain was incorporated as the Fmoc-Lys(Mtt)-OH derivative. The Mtt protection was removed on the peptide synthesizer by treatment with hexafluoroisopropanol and the sidechain functionalized using standard solid-phase Fmoc procedures. The lysine to be modified with a chelator after cleavage from the solid-phase was incorporated as the Fmoc-Lys (Boc)-OH derivative.

Cleavage from the resin was accomplished by shaking the resin with 95% trifluoroacetic acid (TFA), 2.5% water and 2.5% triisopropylsilane (TIPS) for 1.5 h, followed by precipitation in cold diethyl ether (−78 °C).

The peptides were then dissolved in 25% acetonitrile in water and purified by preparative HPLC.

4.2. Peptide modification

The purified peptide as a TFA salt was dissolved in a carbonate buffer (0.10 M Na_2CO_3 and 0.10 M $NaHCO_3$) containing 20% acetonitrile to make a 1.0 M solution. Three equivalents of the desired chelator were added, and the resulting mixture was stirred at 50 °C until judged complete by UPLC analysis (approx. 3 h). The reaction was then neutralized with 13% TFA (aq.) and purified by preparative HPLC. After lyophilization, the peptide was then used in the incorporation, stability and imaging studies with zirconium-89.

For the compounds coordinating non-radioactive zirconium, the metal ion was incorporated by addition of approx. 1.5 equivalents of 0.1 M $ZrCl_4$ (aq.) directly to the preparative HPLC fractions and adjustment of the pH to 8.0 with carbonate buffer. After complete incorporation, the compounds were purified by prep-HPLC and lyophilized to yield the desired peptide. Purities of the modified peptides can be found in the Supplementary Information page S5.

4.3. Animals used for PD, biodistribution and PET

The PD study was carried out in accordance with permission given by the experimental animal committee in Denmark. A total of 32 lean Sprague-Dawley male rats 7–8 weeks old (Taconic, Denmark) were randomized and placed on reversed light-dark (light 11 pm, dark 11 am) cycle in the Biodaq system cages 12 days prior to the start of the study and fed an *ad libitum* Altromin and water diet throughout.

The Dutch central committee on animal research and the local ethical committee on animal research of the Radboud University approved the biodistribution and PET studies under protocol 2017-0028. All animal experiments were performed according to the institutional guidelines by blinded biotechnicians. Upon arrival, 7–8 weeks old male Sprague Dawley® rats (Envigo, Horst, the Netherlands) were randomly marked with a waterproof marker on their tail for identification and were acclimatized for ≥4 days before any experimental procedure.

The number of rats in each group was based on previous experiments to ensure that sufficient animals were used to accurately estimate the radiotracer biodistribution and the food intake. Rats were randomly allocated to the experimental groups and assessed daily for welfare. All rats allocated to one of the experimental groups were used in the final analysis of the data, no rats were excluded. None of the animals suffered from adverse effects during the study.

In all studies, rats had unlimited access to food and water in a controlled environment (22 ± 1 °C, 55 ± 10% humidity, 12 h dark/light cycle). Cages were weekly replaced by clean cages.

4.4. Radiolabelling and stability

7 nmol of the modified peptide**s** were incubated with 35 MBq [^{89}Zr] Zr(oxalate)$_2$] solution adjusted to pH 7.8 with 2 M Na_2CO_3 for 2 h at

37 °C. The radiolabelling was evaluated with instant thin layer chromatography (iTLC) using sialic acid impregnated iTLC strips and NH_4Ac EDTA as mobile phase and showed complete chelation (>98.5%) of the resulting radiolabelled complexes.

4.5. Administration, blood kinetics and biodistribution

Rats (250–300 g, 7–8 weeks old, 5 per group) received an intravenous injection in the tail vein of 1 nmol (5 MBq) **[^{89}Zr]Zr-DFO-4** or **[^{89}Zr]Zr-DFO*-5** in 200 μL vehicle (50 mM phosphate buffer, 70 mM NaCl, 70 ppm Tween20, pH 7.4). A few drops of blood were collected from the vena saphena at 15 min, 30 min, 1 h, 2 h, and 3 h post injection. At 4 or 24 h post injection animals were euthanized by CO_2 asphyxiation and blood and organs (muscle, heart, lung, spleen, liver, pancreas, kidney, stomach, duodenum, colon, femur, knee, bone marrow, brain and skin) were collected for *ex vivo* analysis. Zirconium-89 radioactivity was quantified in collected samples using a gamma counter (Wizard, PerkinElmer) and expressed as the percentage of injected dose per gram tissue (%ID/g), calculated from the amount of radioactivity measured in aliquots of the injected dose.

4.6. PET imaging

Two rats of each group were randomly selected for PET imaging. Euthanized rats were imaged for 20 min at 4 h after injection using an Inveon animal PET scanner (Siemens Preclinical solutions). Reconstruction of scans was performed using Inveon Acquisition Workplace software with an iterative three-dimensional ordered subset expectation maximization using maximum *a priori* with shifted Poisson distribution algorithm with the following parameters: matrix, 256 × 256 × 161; pixel size, 0.4 × 0.4 × 0.8 mm with a corresponding beta of 0.05 mm.

Supplementary data to this article can be found online at https://doi.org/10.1016/j.nucmedbio.2019.11.006.

Declaration of competing interest

The authors declare that they have no conflict of interest.

Acknowledgements

This study received funding from the Innovative Medicines Initiative 2 Joint Undertaking under grant agreement No 116106. This Joint Undertaking received support from the European Union's Horizon 2020 research and innovation program and EFPIA. In addition, this work was supported by the Centre National de la Recherche Scientifique (CNRS), the Université de Bourgogne and the Conseil Régional de Bourgogne Franche-Comté through the Plan d'Action Régional pour l'Innovation^ (program PARI), and by the European Union through the PO FEDER-FSE 2014/2020 Bourgogne program, Netherlands Organisation for Scientific Research (NWO, project number 91617039), and the Dutch Cancer Society (KWF, project number 10099).

References

[1] Meier JJ. GLP-1 receptor agonists for individualized treatment of type 2 diabetes mellitus. Nat Rev Endocrinol 2012;8:728–42.
[2] Kolterman OG, Kim DD, Shen L, Ruggles JA, Nielsen LL, Fineman MS, et al. Pharmacokinetics, pharmacodynamics, and safety of exenatide in patients with type 2 diabetes mellitus. Am J Health Syst Pharm 2005;62:173–81.
[3] Buse JB, Rosenstock J, Sesti G, Schmidt WE, Montanya E, Brett JH, et al. Liraglutide once a day versus exenatide twice a day for type 2 diabetes: a 26-week randomised, parallel-group, multinational, open-label trial (LEAD-6). Lancet 2009;374:39–47.
[4] Bush MA, Matthews JE, De Boever EH, Dobbins RL, Hodge RJ, Walker SE, et al. Safety, tolerability, pharmacodynamics and pharmacokinetics of albiglutide, a long-acting glucagon-like peptide-1 mimetic, in healthy subjects. Diabetes Obes Metab 2009; 11:498–505.
[5] Glaesner W, Vick AM, Millican R, Ellis B, Tschang SH, Tian Y, et al. Engineering and characterization of the long-acting glucagon-like peptide-1 analogue LY2189265, an Fc fusion protein. Diabetes Metab Res Rev 2010;26:287–96.
[6] Lau J, Bloch P, Schaffer L, Pettersson I, Spetzler J, Kofoed J, et al. Discovery of the once-weekly glucagon-like peptide-1 (GLP-1) analogue Semaglutide. J Med Chem 2015; 58:7370–80.
[7] Sun X, Li Y, Liu T, Li Z, Zhang X, Chen X. Peptide-based imaging agents for cancer detection. Adv Drug Deliv Rev 2017;110–111:38–51.
[8] Bauman A, Valverde IE, Fischer CA, Vomstein S, Mindt TL. Development of (68)Ga- and (89)Zr-labelled exendin-4 as potential radiotracers for the imaging of Insulinomas by PET. J Nucl Med 2015;56:1569–74.
[9] Deri MA, Zeglis BM, Francesconi LC, Lewis JS. PET imaging with (89)Zr: from radiochemistry to the clinic. Nucl Med Biol 2013;40:3–14.
[10] Dilworth JR, Pascu SI. The chemistry of PET imaging with zirconium-89. Chem Soc Rev 2018;47:2554–71.
[11] Heskamp S, Raave R, Boerman O, Rijpkema M, Goncalves V, Denat F. (89)Zr-Immuno-positron emission tomography in oncology: state-of-the-art (89)Zr radiochemistry. Bioconjug Chem 2017;28:2211–23.
[12] Wild D, Macke H, Christ E, Gloor B, Reubi JC. Glucagon-like peptide 1-receptor scans to localize occult insulinomas. N Engl J Med 2008;359:766–8.
[13] Pattou F, Kerr-Conte J, Wild D. GLP-1-receptor scanning for imaging of human beta cells transplanted in muscle. N Engl J Med 2010;363:1289–90.
[14] Gotthardt M, Fischer M, Naeher I, Holz JB, Jungclas H, Fritsch HW, et al. Use of the incretin hormone glucagon-like peptide-1 (GLP-1) for the detection of insulinomas: initial experimental results. Eur J Nucl Med Mol Imaging 2002;29:597–606.
[15] Behnam Azad B, Rota VA, Breadner D, Dhanvantari S, Luyt LG. Design, synthesis and in vitro characterization of glucagon-like Peptide-1 derivatives for pancreatic beta cell imaging by SPECT. Bioorg Med Chem 2010;18:1265–72.
[16] Brom M, Woliner-van der Weg W, Joosten L, Frielink C, Bouckenooghe T, Rijken P, et al. Non-invasive quantification of the beta cell mass by SPECT with (111)In-labelled exendin. Diabetologia 2014;57:950–9.
[17] Knudsen LB, Lau J. The discovery and development of liraglutide and semaglutide. Front Endocrinol 2019;10:155.
[18] Knudsen LB, Nielsen PF, Huusfeldt PO, Johansen NL, Madsen K, Pedersen FZ, et al. Potent derivatives of glucagon-like peptide-1 with pharmacokinetic properties suitable for once daily administration. J Med Chem 2000;43:1664–9.
[19] Manandhar B, Ahn JM. Glucagon-like peptide-1 (GLP-1) analogs: recent advances, new possibilities, and therapeutic implications. J Med Chem 2015;58:1020–37.
[20] Rudd SE, Roselt P, Cullinane C, Hicks RJ, Donnelly PS. A desferrioxamine B squaramide ester for the incorporation of zirconium-89 into antibodies. Chem Commun 2016;52:11889–92.
[21] Vosjan MJ, Perk LR, Visser GW, Budde M, Jurek P, Kiefer GE, et al. Conjugation and radiolabeling of monoclonal antibodies with zirconium-89 for PET imaging using the bifunctional chelate p-isothiocyanatobenzyl-desferrioxamine. Nat Protoc 2010; 5:739–43.
[22] Vugts DJ, Klaver C, Sewing C, Poot AJ, Adamzek K, Huegli S, et al. Comparison of the octadentate bifunctional chelator DFO*-p-Phe-NCS and the clinically used hexadentate bifunctional chelator DFO-p-Phe-NCS for (89)Zr-immuno-PET. Eur J Nucl Med Mol Imaging 2017;44:286–95.
[23] Neidigh JW, Fesinmeyer RM, Prickett KS, Andersen NH. Exendin-4 and glucagon-like-peptide-1: NMR structural comparisons in the solution and micelle-associated states. Biochemistry 2001;40:13188–200.
[24] Andersen NH, Brodsky Y, Neidigh JW, Prickett KS. Medium-dependence of the secondary structure of exendin-4 and glucagon-like-peptide-1. Bioorg Med Chem 2002;10:79–85.
[25] Jazayeri A, Rappas M, Brown AJH, Kean J, Errey JC, Robertson NJ, et al. Crystal structure of the GLP-1 receptor bound to a peptide agonist. Nature 2017;546:254–8.
[26] Runge S, Thogersen H, Madsen K, Lau J, Rudolph R. Crystal structure of the ligand-bound glucagon-like peptide-1 receptor extracellular domain. J Biol Chem 2008; 283:11340–7.
[27] Greenfield NJ. Using circular dichroism spectra to estimate protein secondary structure. Nat Protoc 2006;1:2876–90.
[28] Raun K, von Voss P, Gotfredsen CF, Golozoubova V, Rolin B, Knudsen LB. Liraglutide, a long-acting glucagon-like peptide-1 analog, reduces body weight and food intake in obese candy-fed rats, whereas a dipeptidyl peptidase-IV inhibitor, vildagliptin, does not. Diabetes 2007;56:8–15.
[29] Raave R, Sandker G, Adumeau P, Jacobsen CB, Mangin F, Meyer M, et al. Direct comparison of the in vitro and in vivo stability of DFO, DFO* and DFOcyclo* for (89)Zr-immunoPET. Eur J Nucl Med Mol Imaging 2019;46:1966–77.
[30] Patra M, Bauman A, Mari C, Fischer CA, Blacque O, Haussinger D, et al. An octadentate bifunctional chelating agent for the development of stable zirconium-89 based molecular imaging probes. Chem Commun 2014;50:11523–5.
[31] Berg E, Gill H, Marik J, Ogasawara A, Williams S, van Gongen G, et al. Total-body PET and highly stable chelators together enable meaningful (89)Zr-antibody-PET studies up to 30 days postinjection. J Nucl Med 2019. https://doi.org/10.2967/jnumed.119.230961.
[32] Vegt E, Melis M, Eek A, de Visser M, Brom M, Oyen WJ, et al. Renal uptake of different radiolabelled peptides is mediated by megalin: SPECT and biodistribution studies in megalin-deficient mice. Eur J Nucl Med Mol Imaging 2011;38:623–32.
[33] Vegt E, de Jong M, Wetzels JF, Masereeuw R, Melis M, Oyen WJ, et al. Renal toxicity of radiolabelled peptides and antibody fragments: mechanisms, impact on radionuclide therapy, and strategies for prevention. J Nucl Med 2010;51:1049–58.
[34] https://www.ema.europa.eu/en/documents/assessment-report/ozempic-epar-public-assessment-report_en.pdf (accessed on November 19th 2019). On page 24 of the EMA report for a GLP-1 analogue it is stated that: "The terminal half-life was estimated to be 8 h in the mouse, 11 h in the rat, 28 h in the rabbit, 51 h in the monkey and 148 h in human."